

the Ministry of Industry, Science and Technology), and the Ministry of the Russian Federation on Atomic Energy.

## References

1. Goremychkin E A, Osborn R, Taylor A D *Pis'ma Zh. Eksp. Teor. Fiz.* **50** 351 (1989) [*JETP Lett.* **50** 380 (1989)]
2. Temprano D R et al. *Phys. Rev. Lett.* **84** 1990 (2000)
3. Orenstein J, Millis A J *Science* **288** 468 (2000)
4. Reichardt W et al. *J. Supercond.* **7** 399 (1994)
5. Petrov Y et al., cond-mat/0003414
6. Mirmelstein A et al. *J. Phys: Condens. Mat.* **11** 7155 (1999)
7. Kee H-Y, Kivelson S A, Aeppli G, cond-mat/0110478
8. Aksenov V L et al. *High Pressure Res.* **14** 127 (1995); Balagurov A M et al. *Physica C* **275** 87 (1997)
9. Aksenov V L et al. *Phys. Rev. B* **55** 3966 (1997); Balagurov A M et al. *Phys. Rev. B* **59** 7209 (1999)
10. Abakumov A M et al. *Phys. Rev. Lett.* **80** 385 (1998)
11. Lokshin K A et al. *Phys. Rev. B* **63** 064511 (2001)
12. Plakida N M *Pis'ma Zh. Eksp. Teor. Fiz.* **74** 38 (2001) [*JETP Lett.* **74** 36 (2001)]
13. Aksenov V L et al. *Pis'ma Zh. Eksp. Teor. Fiz.* **61** 294 (1995) [*JETP Lett.* **61** 307 (1995)]; Lauter-Pasyuk V et al. *Physica B* **267** 149 (1999)
14. Zabenkin V N et al. *Physica B* **297** 268 (2001)

PACS numbers: **74.50.+p**, **74.62.Dh**, **74.72.-h**  
DOI: 10.1070/PU2002v045n06ABEH001195

## Tunneling and Andreev spectroscopies of high-temperature superconductors

Ya G Ponomarev

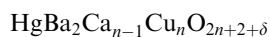
### 1. Introduction

Theoretical and experimental studies of the nature of high-temperature superconductivity are far from completion [1–4]. However, in the 15 years of studies of high-temperature superconductors (HTSC), studies that employed the most modern experimental methods, an enormous body of data has been gathered and theoretical models for describing the unique properties of HTSCs have been built. Note that even today there is no agreement in the choice of the pairing mechanism [5–8], although the existence of an isotopic effect in underdoped and overdoped cuprate superconductors is a clear indication of the important role that phonons play in the formation of the superconducting properties of HTSCs [5].

According to modern ideas [9–11], doped crystals of the cuprate superconducting compounds



and



constitute a natural superlattice of the type SISI... , where S is a thin superconducting block containing one or more  $\text{CuO}_2$  planes intercalated with calcium, and I is a layer of insulator (spacer) that, in particular, actuates doping of the  $\text{CuO}_2$  blocks due to introduction of excess oxygen into the central part of the spacer. Since the dopant is outside the  $\text{CuO}_2$  blocks, it has no significant effect on the hole relaxation time in the  $\text{CuO}_2$  planes. Introduction of impurities (magnetic or nonmagnetic) into the  $\text{CuO}_2$  planes rapidly suppresses superconductivity. In cuprate HTSCs the spacers occupy up to

80% of the crystal's volume, while only about 20% is occupied by the superconducting  $\text{CuO}_2$  blocks. Spacers play an important role in forming the electron transport in the  $c$ -direction due to resonance tunneling [9, 12].

When the temperature is below  $T_c$ , a doped high-temperature superconducting crystal behaves as a stack of strongly coupled Josephson junctions, so that the superconducting current in the  $c$ -direction is of the Josephson nature (weak superconductivity). Note that the specific superconducting properties of layered crystals with Josephson coupling of layers were discussed in detail even before high-temperature superconductivity was discovered (Ref. [13], Chap. 6).

In pure cuprates, a  $\text{CuO}_2$  plane with a half-filled 2D band proves to be unstable against a transition into the Mott insulator phase as a result of formation of long-range antiferromagnetic order (doubling the period causes the area of the 2D Brillouin zone to diminish by a factor of two). Light doping with oxygen destroys the long-range antiferromagnetic order, which leads to an insulator–metal transition and to the emergence of a hole Fermi surface of open type [14]. Here the Fermi level may be in the vicinity of an extended Van Hove singularity with giant peaks in the density of states in  $\Gamma$ –M directions [5, 15].

High-temperature superconductivity occurs in  $\text{CuO}_2$  planes within a relatively narrow interval of impurity hole concentrations  $p$ . The Fermi surface changes only slightly in the process [16]. According to photoemission spectroscopy data, the superconducting gap is largest in the  $\Gamma$ –M direction (i.e. in the direction of a Van Hove singularity) and smallest in the  $\Gamma$ –Y direction, in which the electron density of states passes through a minimum [17]. The gap anisotropy decreases substantially as  $p$  increases [18]. Note that at least in principle the Fermi level may get pinned to a Van Hove singularity within a certain interval of impurity hole concentrations  $p$  [19]. The superconducting transition temperature  $T_c$  varies with  $p$  according to a parabolic law (in the first approximation) [20].

### 2. Some experimental results obtained in HTSC studies using the tunneling and Andreev spectroscopy methods

When applied to HTSC, the methods of tunneling and Andreev (point-contact) spectroscopies demonstrated their efficiency and made it possible to extract useful information about the physical properties of these materials in the superconducting and normal states. Below I briefly discuss some recent experimental results of tunneling and point-contact measurements involving HTSC samples.

#### 2.1 Intrinsic Josephson effect.

##### Characteristic properties of the SISI... structure

An achievement that can be considered really important is the discovery and study in cuprate superconductors of the intrinsic Josephson effect [21–24], which clearly demonstrated the 2D nature of electron transport in HTSC. Thorough investigations of the intrinsic Josephson effect in various high-temperature superconducting materials actually led to the creation of a new method of studying layered superconductors, *the intrinsic tunneling spectroscopy method*.

Studies of the intrinsic Josephson effect in high-temperature superconducting mesostructures fully corroborated the SISI... model: (1) when  $T < T_c$ , multiple-branch current–

voltage characteristics of mesostructures with the current flowing in the  $c$ -direction were discovered [21–24]; (2) the current–voltage characteristics of mesostructures were found to exhibit geometric Fiske resonances [25]; (3) Fraunhofer oscillations of the critical Josephson current as a function of the external magnetic field were discovered [26]; and (4) at currents higher than the critical current  $j_c$  were sent through high-temperature superconducting mesostructures, emission of microwave radiation from the mesostructures was observed [21–23].

## 2.2 Intrinsic Josephson effect.

### Calculating the superconducting gap and evaluating the shape of the current–voltage characteristic

The intrinsic Josephson effect was observed [27, 28] in doped Bi-2212 single crystals on natural ultrathin steps (with a height from 1.5 to 30 nm), which are always present on a cryogenic cleavage surface (the break junction technique). Direct measurements done by the scanning tunneling microscopy (STM) method showed that the height of these steps is proportional to half the height of the unit cell,  $c/2 = 1.5$  nm (the cleavage surface is between two BiO planes) [29, 30]. Note that half a unit cell in the  $c$ -direction corresponds to a single Josephson junction.

According to Kaneko et al. [29] and Mitchell et al. [30], the microstep width does not exceed 1  $\mu\text{m}$ . This result coincides with the estimates made in Ref. [27]. By tuning the junction with a micrometer screw in a single experiment it is possible to move from one step to another and record their current–voltage characteristics individually ( $\mathbf{j} \parallel \mathbf{c}$ ).

The authors of Refs [27, 28] discovered at liquid-helium temperatures a pronounced gap structure in the current–voltage characteristics of the microsteps on the cryogenic cleavage surface in underdoped and optimally doped Bi-2212(La) single crystals and in overdoped Bi-2212 single crystals and whiskers (Fig. 1). Stacks of Josephson junctions with  $1 \leq n \leq 25$  ( $n$  is the number of junctions) were studied. The high resistance of the stacks [ $R_N(4.2 \text{ K}) = 200\text{--}2000 \Omega$  per junction] made it possible to broaden the range of bias voltages to values much higher than the gap voltage  $V_{gn}$  without significant junction overheating. For a stack of  $n$  equivalent junctions, the value of the gap voltage  $V_{gn}$  corresponding to a sharp increase in the quasi-particle current  $\mathbf{j}_{qp} \parallel \mathbf{c}$  is given by the formula  $V_{gn} = (2\Delta/e)n$ . The experimental dependence  $V_{gn}(n)$  can be used to determine the gap parameter  $\Delta$  with high accuracy (see the inset in Fig. 1). For optimally doped BSCCO(La) samples,  $\Delta_{4.2\text{K}} = (27.0 \pm 0.5) \text{ meV}$  at  $T_c = (91 \pm 2) \text{ K}$  and  $2\Delta/kT_c = 6.9 \pm 0.5$ . With the temperature increasing, the gap structure in the current–voltage characteristics of stacks still retains its ‘abrupt’ shape in a wide range of temperatures  $T < T_c$  which makes it possible to determine the temperature dependence of the gap,  $\Delta(T)$ .

It was found (see Ref. [28]) that when the current–voltage characteristics of stacked SIS junctions are plotted in reduced coordinates, they almost coincide. The gap feature in the current–voltage characteristics has a shape typical for an ‘s-symmetry’ (isotropic) gap parameter. At first glance it is difficult to match this result with the photoemission spectroscopy data, according to which the gap parameter in the  $ab$  plane is highly anisotropic [17]. However, the situation changes when there is a van Hove singularity at the Fermi level. Wei et al. [31] found that a van Hove singularity enhances the gap structure in the current–voltage character-

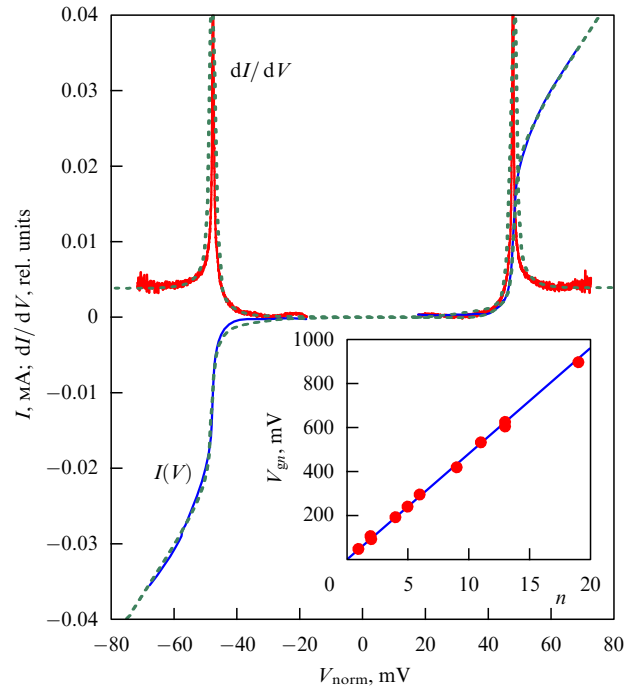


**Figure 1.** Current–voltage characteristic [normalized to a single junction, ( $V_{\text{norm}} = V/n$ )] of a microstep on a cryogenic cleavage in an underdoped Bi-2212(La) single crystal with the number of junctions  $n = 13$  at  $T = 4.2 \text{ K}$  ( $T_c = 81 \pm 3 \text{ K}$ ). The dashed curves represent the results of calculations by the Dynes model with the following values of the parameters per junction:  $\Delta = 24 \text{ meV}$ ,  $\Gamma = 0.5 \text{ meV}$ , and  $R_N = 1700 \Omega$ . The inset shows the dependence obtained in a single experiment of the gap voltage  $V_{gn}$  on the number of SIS junctions,  $n$ , in microsteps of different height.

istics of junctions even when the gap parameter in the  $ab$  plane is highly anisotropic.

## 2.3 Intrinsic Josephson effect. Pseudogap

The poorly pronounced ‘gap’ structure (pseudogap) in the current–voltage characteristics of Bi-2212 mesostructures observed in some cases at temperatures higher than  $T_c$  [32, 33] is not directly related to superconductivity and, possibly, is caused by the fact that the metallic  $\text{CuO}_2$  blocks are two-dimensional. Note that the effect of 2D (surface) bands on the current–voltage characteristics of normal-state tunneling junctions has been theoretically studied by BenDaniel and Duke [34]. The ‘multigap’ structure that they predicted was observed by Mironova et al. [35] in the current–voltage characteristics of normal Bi– $\text{Al}_2\text{O}_3$ –Al junctions over an extremely broad temperature interval.

## 2.4 Josephson spectroscopy.

### Generation in Josephson HTSC junctions of Raman-active (nonpolar) optical phonons by AC Josephson current over a frequency range up to 20 THz

Today there exist a large number of theoretical models (see the reviews [2, 3]) in which the phenomenon of high-temperature superconductivity is described using the phonon mechanism of pairing, modified by the strong Coulomb repulsion.

One such model was recently proposed by Abrikosov [5]. According to him, a high superconducting transition temperature  $T_c$  in HTSC occurs because of the presence near the Fermi level of an extended van Hove singularity with a high

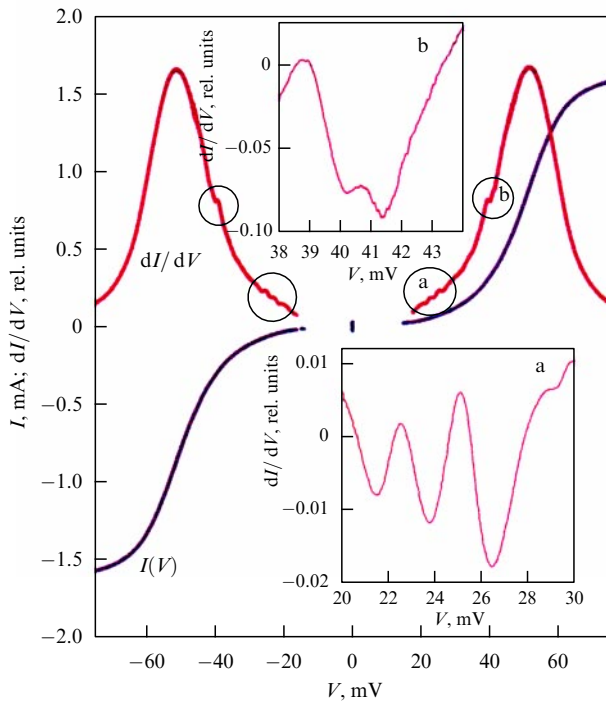


**Figure 2.**  $I(V)$  and  $dI(V)/dV$  characteristics of a Josephson junction on a microcrack in an overdoped Bi-2212 single crystal at  $T = 4.2$  K ( $T_c = 87$  K,  $\Delta = 25.5$  meV). The circles designated a and b represent the structure in the  $dI(V)/dV$  characteristics, which is related to excitation of Raman-active optical phonons by an alternating Josephson current for bias voltages  $V_i = \hbar\omega_i/2e$ . In the insets a and b this structure is shown on an enlarged scale with the monotonic dependence subtracted.

density of states [5, 15, 36]. In Abrikosov's model, optical phonons with small wave vectors play the leading role in pairing. The fact that there is a strong electron-phonon coupling in HTSC was confirmed by studies of the effect of generation of Raman-active optical phonons by AC Josephson current in a frequency range up to 20 THz in Bi-2201, Bi-2212, and Bi-2223 Josephson junctions [37–41] (Fig. 2), by photoemission spectroscopy data [42, 43], and by studies of the isotopic effect [44, 45], and the effect of renormalization of the quasi-particle density of states at temperatures below  $T_c$  [46–48].

Aminov et al. [49] were the first to discover a fine structure in the current-voltage characteristics of Josephson Bi-2212 junctions, related, as it is now clear, to the generation by AC Josephson current of nonpolar optical phonons in the  $\epsilon_{\text{phonon}} = 38\text{--}54$  meV energy range. Later Yurgens et al. [50] and Schlenga et al. [51] studied the current-voltage characteristics of Bi-2212 mesastructures and recorded resonances corresponding to the optical modes related to vibration of the heavy ions of bismuth, strontium, and copper ( $\epsilon_{\text{phonon}} = 6\text{--}24$  meV). A phenomenological theory explaining the interaction of AC Josephson current with IR-active (polar) optical phonons was proposed by Schlenga et al. [51]. A complete theory that incorporated the interaction with all optical modes (Raman-active and IR-active) was developed by Maksimov, Arseyev, and Maslova [41]. In Ref. [37], interaction between AC Josephson current and Raman-active phonon modes in the entire range of phonon frequencies (up to 20 THz), including the apex oxygen mode ( $\epsilon_{\text{phonon}} \approx 80$  meV), was discovered (Fig. 3). The upper part of Fig. 3 depicts fragments of the resonance

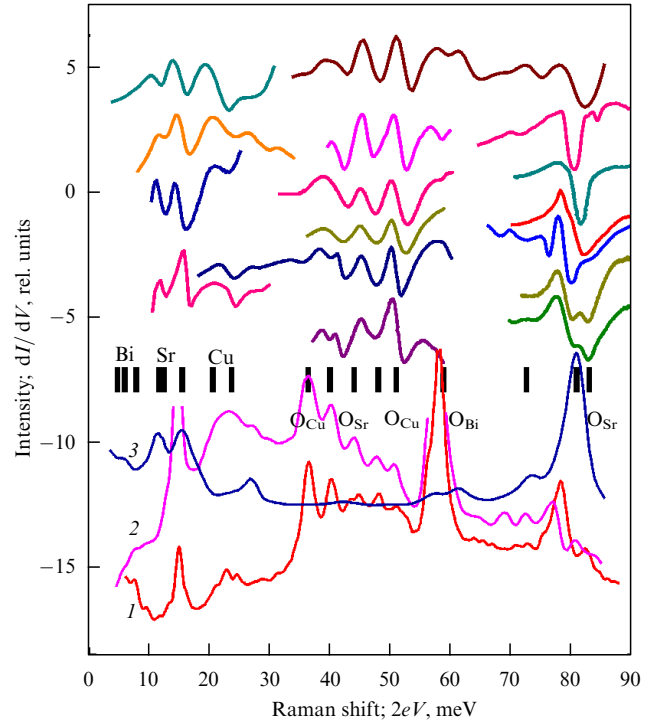


**Figure 3.** Comparison of the structure in the  $dI(V)/dV$  characteristics of Josephson Bi-2212 junctions, which is caused by excitation of optical phonons by an alternating Josephson current, with the Raman phonon spectra in Bi-2212 (see the main text).

structure (plotted against  $2eV$ ) in the  $dI/dV$  characteristics of several break junctions in Bi-2212 single crystals (with the doping close to optimal) at  $T = 4.2$  K. The structure can be observed in the energy range  $0 \leq 2eV \leq 85$  meV, which encompasses the range within which Raman-active optical phonons in Bi-2212 exist. Note that the resonances comprising the structure appear for bias voltages  $V$  satisfying the condition  $2eV = \hbar\omega_{\text{phonon}}$ . For the sake of comparison, in the lower part of Fig. 3 I have placed the results of measurements of Raman spectra for Bi-2212 [52] in two main polarizations (curves 1 and 2 correspond to the  $z(x, x)z$ -geometry, and curve 3 to the  $y(z, z)y$ -geometry). The short lines in the central part of Fig. 3 indicate the energies of Raman-active phonons related to the vibration of atoms belonging to the Bi-2212 structure (see Table 1 in Ref. [37]).

Further experimental studies of low-frequency phonon resonances (Bi-, Sr-, and Cu-optical modes) in the current-voltage characteristics of break junctions in Bi-2201(La) single crystals have shown that AC Josephson current generates optical phonons not only in SIS junctions but also in SNS junctions [40] (N stands for a normal-metal layer), thus fully corroborating the validity of the Maksimov-Arseyev-Maslova model [41]. It has also been found that in the current-voltage characteristics of doped-Bi2212(La) Josephson junctions the structure related to generation of optical phonon modes can be observed in both underdoped and overdoped single crystals, with the doping level having only a small effect on the frequency of the main phonon modes [40]. The latter remark means that the strength of the electron-phonon coupling in BSCCO does not significantly change over the entire region where superconductivity exists.

Studies of the intrinsic Josephson effect in microsteps on a cryogenic cleavage surface of BSCCO with a small number of SIS junctions have shown (see Ref. [40]) that in some cases the generation of nonequilibrium optical phonons is of a synchronized nature. We also note that Bi-2201(La) samples with doping close to optimal exhibit [40] temperature anomalies in the  $2\Delta$  optical Cu-phonon mode ( $\varepsilon_{\text{phonon}} = 2\Delta$ ) at temperatures below  $T_c$ . These anomalies could be related to renormalization of the spectrum of optical phonons with  $k \rightarrow 0$  and with frequencies close to  $2\Delta(0)$  for HTSC with strong electron–phonon coupling at temperatures below  $T_c$  (the renormalization was predicted by Zeyer and Zwicknagl [53] and by Karakozov and Maksimov [54]). Depending on the value of the ratio  $\omega_0/2\Delta$ , where  $\omega_0$  is the phonon frequency at  $T > T_c$ , as the temperature lowers in the region  $T < T_c$ , the phonon frequency must either anomalously increase ( $\omega_0/2\Delta > 1$ ) or anomalously decrease (‘soften’) ( $\omega_0/2\Delta \leq 1$ ).

## 2.5 Andreev, tunneling, and intrinsic spectroscopies.

### Effect of doping on the superconducting gap $\Delta$ in bismuth cuprates

The alternative of phonon pairing in HTSC is pairing on spin fluctuations whose amplitude must be at its maximum near the Mott-insulator–superconductor phase transition [4]. Fairly recently Deutscher [55] suggested that underdoped cuprate HTSCs with magnon pairing have two gap energies,  $\Delta_p$  and  $\Delta_s$ . The larger gap (the pseudogap)  $\Delta_p$  existing in a broad temperature interval  $T < T^*$  (this gap can be measured by employing the photoemission or tunneling spectroscopy methods) determines the binding energy  $2\Delta_p$  of the Cooper pairs that remain in the incoherent state when  $T > T_c$ . The smaller gap  $\Delta_s$  (the superconducting gap), which can be measured by the Andreev or Raman spectroscopy methods, determines the minimum energy  $2\Delta_s$  of excitation of the superconducting condensate when  $T < T_c$  ( $T_c < T^*$  in underdoped samples). According to Deutscher’s model [55], the superconducting gap  $\Delta_s$  varies with hole concentration  $p$  in a way similar to  $T_c$ , passing through a maximum when the doping is optimal ( $\Delta_s$  scales with  $T_c$ ). At the same time,  $\Delta_p$  monotonically increases as  $p \rightarrow 0$  (i.e. in the transition from overdoped samples to underdoped).

Even today the nature of the pseudogap  $\Delta_p$  is unclear. There are theoretical models in which the presence of the pseudogap  $\Delta_p$  is related to the presence of incoherent Cooper pairs at  $T > T_c$ , which must lead to the emergence of an excess current in the current–voltage characteristics of junctions of the SN and SNS types [56]. However, an experimental check of this prediction that used NS point contacts (gold–YBCO) produced negative results [57].

Note that the model in which  $\Delta_s$  scales with  $T_c$  on doping of HTSC was challenged by researchers who mainly used the STM method [58–61]. At the same time, thorough investigations have shown (see Refs [62–64]) the *validity* of the scaling model [55] (at least for bismuth cuprates).

The results of measurements of the current–voltage characteristics of Josephson HTSC break junctions in a broad temperature interval extending to the critical temperature  $T_c$  can be found in Refs [62–64]. The following samples were used for the investigations:

- (1) underdoped (UND), optimally doped (OPD), and overdoped (OVD) Bi-2201(La) single crystals;
- (2) UND and OPD Bi-2212(La) single crystals and OVD Bi-2212 single crystals and whiskers.

The following experimental methods were employed in these investigations:

- (1) Andreev spectroscopy (multiple Andreev reflections in break junctions of the SnS type);
- (2) tunneling spectroscopy (single tunneling SIS junctions);
- (3) intrinsic tunneling spectroscopy (intrinsic Josephson effect in microsteps on the cryogenic cleavage surface).

All these methods of investigating the superconducting properties of HTSC involve using break junctions in HTSC single crystals and whiskers. The transition from one measurement mode to another was done by mechanically tuning the break junction at the liquid-helium temperature.

Note that there are substantial specific difficulties in fabricating *single* tunneling HTSC junctions with  $\mathbf{j} \parallel \mathbf{c}$ , difficulties related to the layered nature of the structure of cuprate samples (in the  $c$ -direction the banks of a tunneling junction are themselves a natural stack of Josephson SIS junctions). The superconducting current in the  $c$ -direction at the surface of samples (especially of underdoped samples) is often suppressed. A single  $\text{CuO}_2$  block is unable to completely screen an external electric field in the  $c$ -direction, because the screening length is larger than the thickness of the block [65]. In this case, in series with the main (planned) junction a number of highly nonequivalent additional SIS junctions appear, which may lead to a shift in the total gap structure in the current–voltage characteristic towards higher bias voltages. This effect has been repeatedly observed in underdoped samples [62–64]. To reject the current–voltage characteristics of such complex junctions, researchers use (see Refs [62–64]) phonon resonances, whose existence in  $dI/dV$  characteristics is easily noticeable in the presence of AC Josephson current. These resonances served as reliable calibration marks in current–voltage characteristics which made it possible to distinguish a true single junction from a complex composite junction. As noted in Section 2.4, bias voltages at which current–voltage characteristic acquire features associated with the interaction of AC Josephson current and optical phonons are determined by the condition  $2eV = \hbar\omega_{\text{phonon}}$ . For stack junctions this condition is replaced by  $2eV/n = \hbar\omega_{\text{phonon}}$ .

Note that the above difficulties are, possibly, the reason why in Refs [58–61] the gap size in underdoped Bi-2212 samples is overvalued.

In Refs [62–64] the gap structure in  $dI/dV$  characteristics of a junction in the tunneling regime (the peak value of the differential conductance for a gap voltage  $V_g = 2\Delta/e$ ) is compared to the subharmonic gap structure in the  $dI/dV$  characteristic of the same junction in the point-contact (Andreev) mode (a series of dips in the differential conductance for bias voltages  $V_n = 2\Delta/en$ , where  $n$  is an integer). Earlier Muller et al. [66] did the same type of research with niobium break junctions. The value of the superconducting gap was assumed reliable only if the values of  $\Delta$  obtained by the above two methods were equal. The data of tunneling, intrinsic tunneling, and Andreev spectroscopies were used to build the dependence of the superconducting gap  $\Delta$  on the impurity hole concentration  $p$  in Bi-2212 (Fig. 4).

Figure 4 shows that in Bi-2212 the superconducting gap  $\Delta$  ( $T = 4.2$  K) (solid circles) scales with the superconducting transition temperature  $T_c$  (solid curve) in the entire doping range. The dependence of the superconducting gap  $\Delta$  on the

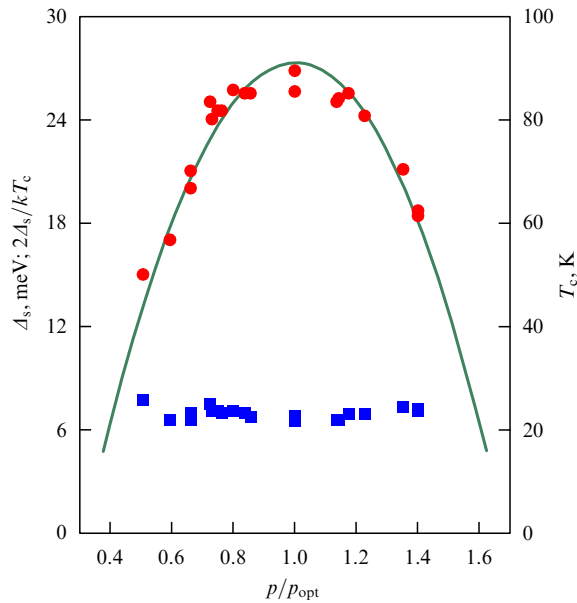
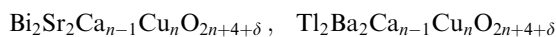


**Figure 4.** Superconducting gap  $\Delta_s$  and the ratio  $2\Delta_s/kT_c$  as functions of the reduced impurity hole concentration  $p/p_{\text{opt}}$  in Bi-2212.

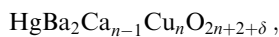
impurity hole concentration  $p$  in Bi-2212 exhibits a small flat section in the optimal doping region (see Fig. 4), which, apparently is the result of pinning of the Fermi level to a van Hove singularity. The ratio  $2\Delta/kT_c = 7.0 \pm 0.5$  (black squares) is, to the first approximation, independent of the doping level. A similar behavior of the superconducting gap was also discovered for Bi-2201 [62–64], but for the ratio  $2\Delta/kT_c \approx 12$ . These results contradict the results of Refs [58–61], according to which the superconducting gap  $\Delta$  for underdoped Bi-2212 samples rapidly grows with decreasing  $T_c$ , so that the value of  $2\Delta/kT_c$  reaches 20 or even higher values.

In Refs [62–64] it was also shown that the gap determined by tunneling and microjunction spectroscopies vanishes in the region of zero resistivity in the resistive transition (i.e. at  $T = T_c$ ) in UND, OPD, and OVD in samples of the Bi-2212 and Bi-2201 phases. This result contradicts the common viewpoint according to which the superconducting gap in underdoped samples is temperature-independent and at  $T = T_c$  becomes a pseudogap of the same size [60].

In conclusion it must be noted that for optimally doped samples of the cuprate families



and



$1 \leq n \leq 3$ , the superconducting gap  $\Delta$  was found (see Ref. [67]) to increase linearly with the number  $n$  of  $\text{CuO}_2$  planes in the superconducting blocks (Fig. 5). In Figure 5 the solid symbols represent the data of Ref. [67], the open triangles represent the data of Ref. [31], the open square the data of Ref. [68], and the open square with the ‘plus’ sign the data of Ref. [69]. Note that the  $n$ -dependence of the maximum critical temperature  $T_{c,\text{max}}$  for cuprates does not obey a simple linear law [70].

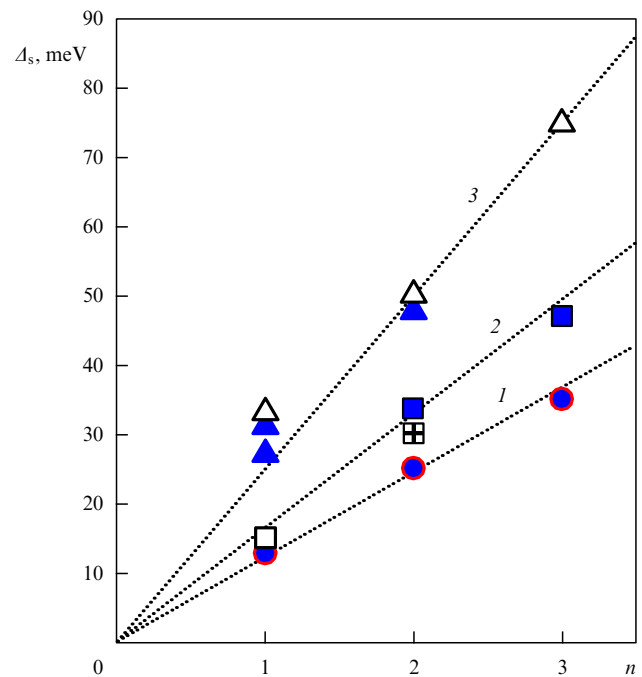


**Figure 5.** Superconducting gap  $\Delta_s(T = 4.2 \text{ K})$  as a function of the number  $n$  of  $\text{CuO}_2$  planes for optimally doped single crystals of the following families:  $\text{Bi}_2\text{Sr}_2\text{Ca}_{n-1}\text{Cu}_n\text{O}_{2n+4+\delta}$  (1),  $\text{Tl}_2\text{Ba}_2\text{Ca}_{n-1}\text{Cu}_n\text{O}_{2n+4+\delta}$  (2), and  $\text{HgBa}_2\text{Ca}_{n-1}\text{Cu}_n\text{O}_{2n+2+\delta}$  (3).

## 2.6 Andreev and intrinsic tunneling spectroscopies.

### Determining the superconducting gap $\Delta$ in $\text{MgB}_2$

Doubts in the universal nature of the magnon pairing mechanism in HTSC appeared after the report of the discovery of a new superconductor, magnesium diboride  $\text{MgB}_2$ , with a critical temperature  $T_c = 39 \text{ K}$  [71]. The pairing mechanism in  $\text{MgB}_2$  is of phonon nature, which is indicated by the discovery in this compound of an isotopic effect in boron [72]. Theoretical analysis of the band structure of  $\text{MgB}_2$  and related compounds shows the conduction along the boron planes is close to two-dimensional ( $\sigma$ -bands) [73]. The presence of a van Hove singularity in the 2D band may strongly affect the value of  $T_c$  if one shifts the Fermi level to the peak in the quasi-particle density of states through doping [74].

According to a popular version [73, 75], magnesium diboride displays two-gap superconductivity, and at  $T = 4.2 \text{ K}$  the gap  $\Delta_{\text{large}} \cong 7 \text{ meV}$  corresponds to the 2D charge carriers in the  $\sigma$ -bands, while the gap  $\Delta_{\text{small}} \cong 2 \text{ meV}$  corresponds to 3D carriers in the  $\pi$ -bands. Calculations have shown that both gaps close simultaneously at the critical temperature  $T_c \cong 40 \text{ K}$ , with the temperature dependence of the gaps close to the standard BCS dependence. The theoretical quasi-particle density of states has two distinctive gap singularities, which must result in two independent subharmonic gap structures, corresponding to  $\Delta_{\text{large}}$  and  $\Delta_{\text{small}}$ , appearing in the current–voltage characteristics of Andreev point contacts of SnS type. This assumption has been recently corroborated at Lomonosov Moscow State University (MSU) by a group of researchers [76], who compared through experiments the temperature dependence of the superconducting gap of polycrystalline  $\text{MgB}_2$  samples (the BG series,  $T_{c,\text{init}} = 39 \text{ K}$ ,  $T_{c,\text{fin}} = 29 \text{ K}$ ) containing up to 20% of  $\text{MgO}$  as an impurity (B M Bulychev and V K Genchel’, Chemical Department of MSU) with the temperature

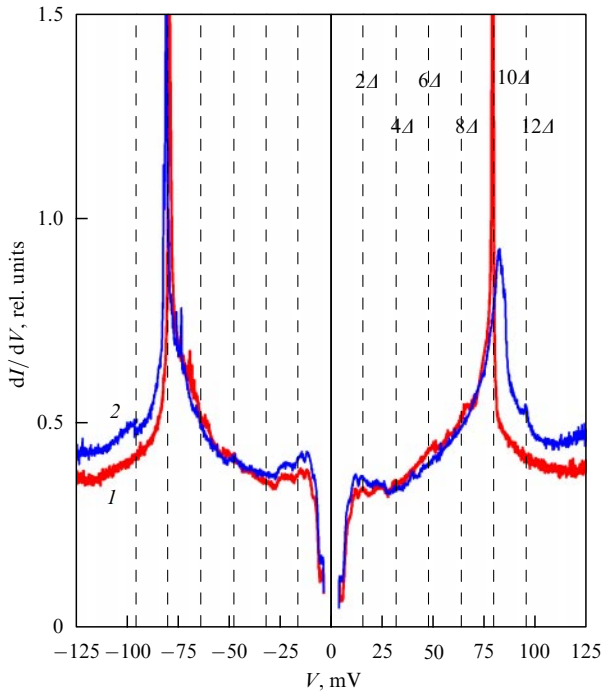


**Figure 6.** Curves 1 and 2 represent the  $dI(V)/dV$  characteristics of stacks of five SIS junctions in  $\text{MgB}_2$  at  $T = 4.2$  K (intrinsic Josephson effect,  $T_c = 32.0 \pm 0.5$  K,  $\Delta_{\text{large}} = 8.0 \pm 0.3$  meV).

dependence of the superconducting gap of polycrystalline  $\text{MgB}_2$  samples (the KV series,  $36 \text{ K} \leq T_c \leq 40 \text{ K}$ ,  $\Delta T = 0.3$  K) containing an excess of magnesium (S I Krasnovobodtsev and A V Varlashkin, P N Lebedev Physics Institute of the Russian Academy of Sciences).

It was found [76] that when the  $\text{MgB}_2$  junctions are put in tunneling regime, the current–voltage characteristics are those typical of the intrinsic Josephson effect (Fig. 6; a stack of five SIS junctions short-circuited by one external SIS junction,  $\Delta_{4.2\text{K}} = 8.0 \pm 0.3$  meV; an alternative explanation of the structure in Fig. 6 is the presence of two-gap conductivity [73, 75]). Until recently, the intrinsic Josephson effect was observed only in cuprate HTSC.

In our work [76], the current–voltage characteristics of more than 150 Andreev point contacts of the SnS type were studied in the temperature interval from 4.2 K to  $T_c$ . The size of the gap was determined from the subharmonic gap structure. We built histograms representing the dependence of the number of junctions on the value of the superconducting gap at 4.2 K for the BG and KV series of samples. Both histograms exhibit peaks at three values of the gap:  $\Delta_1$ ,  $\Delta_2$ , and  $\Delta_3$ . In the case of the BG series,  $\Delta_1 = (2.5 \pm 0.5)$  meV,  $\Delta_2 = (8.0 \pm 0.5)$  meV, and  $\Delta_3 = (16.0 \pm 0.5)$  meV; in the case of the KV series,  $\Delta_1 = (2.5 \pm 0.5)$  meV,  $\Delta_2 = (10.5 \pm 0.5)$  meV, and  $\Delta_3 = (21.0 \pm 0.5)$  meV. According to our interpretation, the gap  $\Delta_2$  corresponds to  $\Delta_{\text{large}}$  [73, 75] and the gap  $\Delta_3$  to  $2\Delta_{\text{large}}$ , which is possible in the case of a stack of two Andreev junctions (the consequence of the layered structure of  $\text{MgB}_2$ ). The gap  $\Delta_1$  corresponds to  $\Delta_{\text{small}}$  [73, 75].

The temperature dependence of the gap in the region near the  $\Delta_2$  peak in the histograms ( $\Delta_{\text{large}}$ ) is described by the BCS model, with the ratio  $2\Delta_2/kT_c$  amounting to  $6.0 \pm 0.5$  for the BG series and  $6.5 \pm 0.5$  for the KV series (Fig. 7). The values are close to  $2\Delta/kT_c$  in superconducting cuprates. The

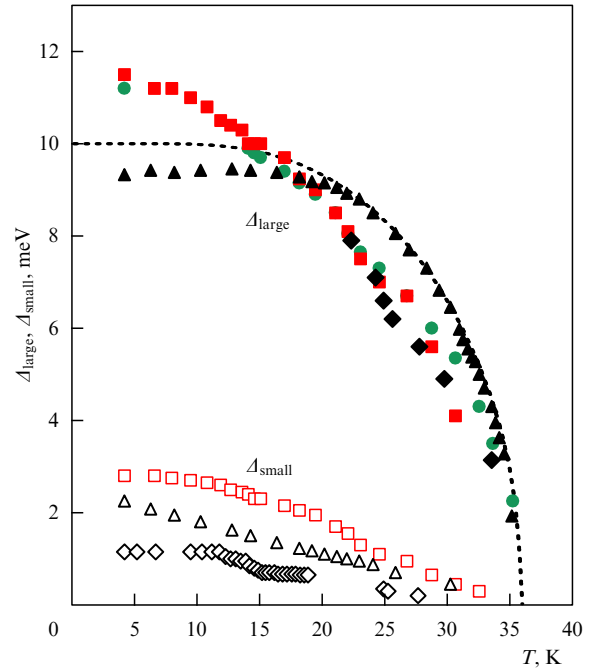


**Figure 7.** Temperature dependence of the large  $\Delta_{\text{large}}$  (solid and hatched symbols) and small  $\Delta_{\text{small}}$  (open symbols) superconducting gaps in three polycrystalline  $\text{MgB}_2$  samples of the KV series with  $T_c = 36$  K (squares and circles refer to the KR6A sample, diamonds refer to the KR6B sample, and triangles to the KRMSUA sample).

temperature dependence of the small gap  $\Delta_{\text{small}}$  (the  $\Delta_1$  peak in the histograms) differs substantially from that supplied by the BCS model, and the ratio  $\Delta_2/\Delta_1$  has no fixed value. The above factors suggest that band-to-band scattering ( $\sigma-\pi$  transitions) greatly affects the size of the small gap  $\Delta_{\text{small}}$  [73].

### Acknowledgements

I would like to thank V F Gantmakher, Yu M Kagan, E G Maksimov, and L M Fisher for their extremely useful discussions of the results of the present research. The work was made possible by partial financial support from the Scientific Council of the Russian ANFKS state-sponsored R&D program (the ‘Delta’ Project) and the Russian Foundation for Basic Research (Grant No. 02-02-17915).

### References

- Ginzburg V L *Usp. Fiz. Nauk* **170** 619 (2000) [*Phys. Usp.* **43** 573 (2000)]
- Maksimov E G *Usp. Fiz. Nauk* **170** 1033 (2000) [*Phys. Usp.* **43** 965 (2000)]
- Kulić M L *Phys. Rep.* **338** 1 (2000)
- Izyumov Yu A *Usp. Fiz. Nauk* **169** 225 (1999) [*Phys. Usp.* **42** 215 (1999)]
- Abrikosov A A, cond-mat/9912394; *Physica C* **341–348** 97 (2000)
- Alexandrov A S, cond-mat/0104413; Alexandrov A S, Sricheewin C, cond-mat/0102284 (v2)
- Varelogiannis G *Physica C* **317–318** 238 (1999)
- Pines D *Tr. J. Phys.* **20** 535 (1996)
- Abrikosov A A *Physica C* **317–318** 154 (1999)
- Bulaevskii L N *Tr. J. Phys.* **20** 594 (1996)
- Bouvier J, Bok J *Physica C* **249** 117 (1995); Bok J, Bouvier J *J. Supercond.* **13** 781 (2000)
- Abrikosov A A *Phys. Rev. B* **55** 11735 (1997)
- Ginzburg V L, Kirzhnits D A (Eds) *Problema Vysokotemperaturnoi Sverkhprovodimosti* (Moscow: Nauka, 1977) [Translated into Eng-

- lish: *High-Temperature Superconductivity* (New York: Consultants Bureau, 1982)]
14. Abrikosov A A *Phys. Rev. B* **64** 104521 (2001)
  15. Gofron K et al. *Phys. Rev. Lett.* **73** 3302 (1994)
  16. Ding H et al. *Phys. Rev. Lett.* **78** 2628 (1997); Timusk T, Statt B *Rep. Prog. Phys.* **62** 61 (1999)
  17. Shen Z-X, Dessau D S *Phys. Rep.* **253** 1 (1995)
  18. Vobornik I et al. *Physica C* **317**–**318** 589 (1999)
  19. Markiewicz R S, Kusko C, Kidambi V *Phys. Rev. B* **60** 627 (1999)
  20. Tallon J L, Williams G V M, Loram J W *Physica C* **338** 9 (2000)
  21. Kleiner R, Müller P *Phys. Rev. B* **49** 1327 (1994); Schlenga K et al. *Phys. Rev. B* **57** 14518 (1998)
  22. Kleiner R, Müller P *Physica C* **293** 156 (1997)
  23. Heim S et al., cond-mat/0107463
  24. Yurgens A A *Supercond. Sci. Technol.* **13** R85 (2000)
  25. Krasnov V M et al. *Phys. Rev. B* **59** 8463 (1999)
  26. Yamashita T et al. *Physica C* **335** 219 (2000)
  27. Ponomarev Ya G et al. *Physica C* **315** 85 (1999)
  28. Ponomarev Ya G et al., in *5th Intern. Workshop "High-Temperature Superconductivity and Novel Inorganic Materials Engineering" (MSU-HTSC-V), Moscow, Russia, 1998* (Abstracts) S-58
  29. Kaneko S et al. *Surf. Sci.* **438** 353 (1999)
  30. Mitchell C E J et al. *Surf. Sci.* **433**–**435** 728 (1999)
  31. Wei J Y T et al. *Phys. Rev. B* **57** 3650 (1998)
  32. Suzuki M, Watanabe T, Matsuda A *Phys. Rev. Lett.* **82** 5361 (1999); Suzuki M, Watanabe T *Phys. Rev. Lett.* **85** 4787 (2000)
  33. Krasnov V M et al. *Phys. Rev. Lett.* **86** 2657 (2001); cond-mat/0002172; *Phys. Rev. Lett.* **84** 5860 (2000)
  34. BenDaniel D J, Duke C B *Phys. Rev.* **152** 683 (1966); **160** 679 (1967)
  35. Mironova G A, Ponomarev Ya G, Roshta L *Fiz. Tverd. Tela (Leningrad)* **17** 906 (1975)
  36. Sherman E Ya, Misochko O V *Phys. Rev. B* **59** 195 (1999)
  37. Ponomarev Ya G et al. *Solid State Commun.* **111** 513 (1999)
  38. Ponomarev Ya G et al., in *5th Intern. Workshop "High-Temperature Superconductivity and Novel Inorganic Materials Engineering" (MSU-HTSC-V), Moscow, Russia, 1998* (Abstracts) S-59
  39. Lorenz M A et al. *J. Low Temp. Phys.* **117** 527 (1999)
  40. Ponomarev Ya G et al., in *XXXI Soveshch. po Fizike Nizkikh Temperatur, Moscow, 1998* (Tez. Dokladov) (31st Workshop on Low-Temperature Physics (Abstracts)) p. 228
  41. Maksimov E G, Arseyev P I, Maslova N S *Solid State Commun.* **111** 391 (1999)
  42. Lanzara A et al., cond-mat/0102227; *Nature* **412** 510 (2001)
  43. Shen Z-X, Lanzara A, Nagaosa N, cond-mat/0102244 (v2)
  44. Zhao G M et al. *Nature* **385** 236 (1997)
  45. Franck J P et al. *Phys. Rev. B* **44** 5318 (1991)
  46. Vedenev S I et al. *Physica C* **235**–**240** 1851 (1994)
  47. Shimada D et al. *Physica C* **298** 195 (1998)
  48. Gonnelli R S, Ummerino G A, Stepanov V A *Physica C* **275** 162 (1997)
  49. Aminov B A et al., in *Superconducting Devices and Their Applications: Proc. of the 4th Intern. Conf. SQUID'91, Berlin, FRG, 1991* (Springer Proc. in Phys., Vol. 64, Eds H Koch, H Lübbig) (Berlin: Springer-Verlag, 1992) p. 45
  50. Yurgens A et al. *Proc. SPIE* **2697** 433 (1996)
  51. Schlenga K et al. *Phys. Rev. Lett.* **76** 4943 (1996); Helm Ch et al. *Phys. Rev. Lett.* **79** 737 (1997); cond-mat/9909318
  52. Boekholt M, Hoffmann M, Güntherodt G *Physica C* **175** 127 (1991); Gasparov L, Güntherodt G, unpublished; Kendziora C, Kelley R J, Onellion M *Phys. Rev. Lett.* **77** 727 (1996)
  53. Zeyer R, Zwicky G Z. *Phys. B: Cond. Mat.* **78** 175 (1990)
  54. Karakozov A E, Maksimov E G *Zh. Eksp. Teor. Fiz.* **115** 1799 (1999) [*JETP* **88** 987 (1999)]
  55. Deutscher G *Nature* **397** 410 (1999)
  56. Choi H-Y, Bang Y, Campbell D K *Phys. Rev. B* **61** 9748 (2000)
  57. Dagan Y et al. *Phys. Rev. B* **61** 7012 (2000)
  58. Ozyuzer L et al. *Physica C* **341**–**348** 927 (2000)
  59. Miyakawa N et al. *Phys. Rev. Lett.* **83** 1018 (1999)
  60. Renner Ch et al. *Phys. Rev. Lett.* **80** 149 (1998)
  61. Oda M et al. *Int. J. Mod. Phys. B* **13** 3605 (1999)
  62. Ponomarev Ya G et al., in *Applied Superconductivity 1999: Proc. of EUCAS 1999, Sitges, Spain, 1999* (Inst. Phys. Conf. Ser., N 167, Eds X Obradors, F Sandiumenge, J Fontcuberta) (Philadelphia, P.A.: Institute of Physics Publ., 2000) p. 241
  63. Schmidt H et al., in *6th Intern. Conf. on Materials and Mechanisms of Superconductivity and High-Temperature Superconductors: M2S-HTSC-VI, February 20–25, 2000, Houston, Texas, USA* (Abstracts) 2C2.6, p. 170; <http://m2s-conf.uh.edu/abstracts/2C2.html>
  64. Timergaleev N Z, in *XXXII Vseross. Soveshch. po Fizike Nizkikh Temperatur, 3–6 Oktyabrya 2000* [Tez. Dokladov] (32nd National Workshop on Low-Temperature Physics, October 3–6, 2000 (Abstracts)] SCP30, p. 104
  65. Machida M, Koyama T, Tachiki M *Phys. Rev. Lett.* **83** 4618 (1999)
  66. Muller C J et al. *Physica C* **191** 485 (1992)
  67. Ponomarev Ya G et al., in *Applied Superconductivity 1999: Proc. of EUCAS 1999, Sitges, Spain, 1999* (Inst. Phys. Conf. Ser., N 167, Eds X Obradors, F Sandiumenge, J Fontcuberta) (Philadelphia, P.A.: Institute of Physics Publ., 2000) p. 245
  68. Tsai J S et al. *Physica C* **162**–**164** 1133 (1989)
  69. Moreland J et al. *Appl. Phys. Lett.* **55** 1463 (1989)
  70. Phillips J C *Phys. Rev. Lett.* **72** 3863 (1994)
  71. Nagamatsu J et al. *Nature* **410** 63 (2001)
  72. Bud'ko S L et al. *Phys. Rev. Lett.* **86** 1877 (2001)
  73. Liu A Y, Mazin I I, Kortus J, cond-mat/0103570; *Phys. Rev. Lett.* **87** 087005 (2001); Mazin I I et al., cond-mat/0204013
  74. Neaton J B, Perali A, cond-mat/0104098
  75. Choi H J et al., cond-mat/0111183
  76. Kuz'michev S A et al., in *Tez. Dokladov Mezhdunarodnoy Konf. Studentov i Aspirantov po Fundamental'nyim Naukam 'Lomonosov-2002', Moskva, 9–12 Aprelya 2002* (Abstracts of the 'Lomonosov-2002' Intern. Conf. of Students and Postgraduates in Fundamental Sciences, Moscow, April 9–12, 2002) (Moscow: Izd. MGU, 2002) p. 433

PACS numbers: 74.20.Mn, 74.20.Rp, 74.62.Dh  
DOI: 10.1070/PU2002v045n06ABEH001196

## High-temperature superconductivity models

Yu V Kopaev

### 1. Introduction

Cuprate-based high-temperature superconductors exhibit special properties in both normal and superconducting states, namely,

- (1) a high superconducting transition temperature  $T_c$ ;
- (2) d-type symmetry of the superconducting order parameter  $\Delta$  and low sensitivity to scattering on nonmagnetic impurities;

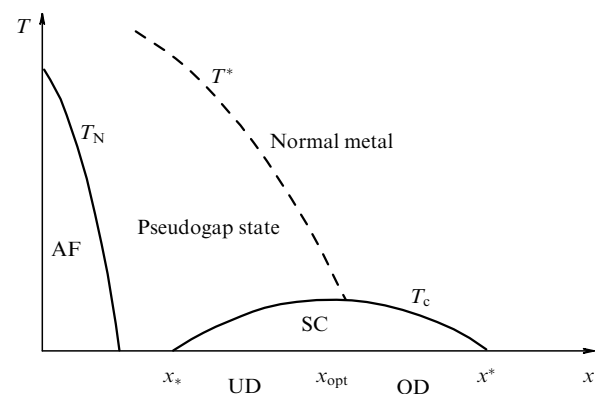


**Figure 1.** Phase diagram typical of hole-doped high-temperature cuprates (temperature vs. doping level  $x$ ). UD and OD stand for the underdoped and overdoped regions, respectively.